

LATERAL DISTRIBUTION OF THE ENERGY FLUX OF THE ELECTRON-PHOTON
COMPONENT OF EXTENSIVE AIR SHOWERS

V. A. DMITRIEV, G. V. KULIKOV, E. I. MASSALSKIĬ, and G. B. KHRISTIANSEN

Nuclear Physics Institute, Moscow State University

Submitted to JETP editor September 15, 1958

J. Exptl. Theoret. Phys. (U.S.S.R.) **36**, 992-1000 (April, 1959)

Measurements are reported on the lateral energy flux distribution of the electron-photon component of extensive air showers with a total number of particles between 1×10^4 to 2×10^6 at sea level. The lateral distribution of the energy flux in the central region of the shower is found to agree with the calculations based on the cascade theory with age parameter of $s = 1.2$. It is shown that the energy flux of the electron-photon component decreases with the distance from the shower axis slower than the energy flux of the nuclear-active component.

The energy carried by the electron-photon component in the central region of the showers is estimated.

INTRODUCTION

NUMEROUS experiments have been devoted to the study of the electron-photon component of extensive air showers (EAS).^{*} In the majority of these, the lateral distribution function of electrons was studied, but only in few experiments^{3,4,5} were the energy characteristics of the soft component investigated.

In the present experiment, the energy flux of the electron-photon component was measured by means of studying the ionization produced by it in a substance with high Z . As is well known, the total energy of the electron-photon component is ultimately dissipated on ionization of the medium and, consequently, if the area under the transition curve of the ionization is known, then one can determine the value of the energy flux carried by the electron-photon component:

$$\rho_E = \int_0^{\infty} n(t) \beta dt,$$

where $n(t)$ is the number of particles at the depth t , and β is the mean energy loss per radiation length. In order to obtain the transition curve, the ionization produced by the electron-photon component under layers of lead of various thickness was studied, using large ionization chambers.

The use of ionization chambers with large area makes it possible to substantially increase the statistical accuracy of the results, and to study

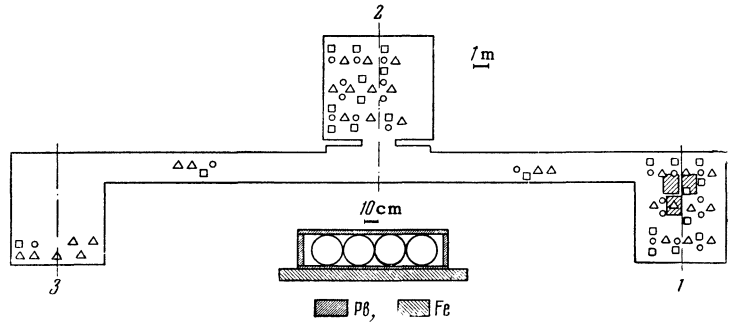
the energy flux of the electron-photon component over a wide range of shower sizes and of distances from the shower axis. Preliminary results of the experiment are given below. The measurements were carried out between June 1957 and February 1958, using the array for comprehensive study of EAS operating at present at Moscow State University.

DESCRIPTION OF THE APPARATUS

For the study of the electron-photon component of EAS, cylindrical ionization chambers, 25 cm in diameter and 1 m long, with a total effective area of 3 m^2 , were used. The chambers were filled with high-purity argon to a pressure of 5 atmos. The thicknesses chosen for the lead absorbers were 2, 4, and 6 cm; in a part of the experiments, the absorber above the chambers was removed. A lead layer 1 cm thick was placed below the chambers. Thus, the chambers were surrounded on all sides by absorbers made of the same substance (see Fig. 1). During almost the whole period of operation of the array, absorbers of various thicknesses were placed above the different chambers. In this way, data about ionization under two different thicknesses of lead were obtained simultaneously for a single shower. The study of a large size range of the showers (1×10^4 to 2×10^6) and, simultaneously, a large range of distances from the shower axis (1 to 50 m, see below) necessitates the recording of ionization varying by a factor of 10,000. This required suitable electronic apparatus which could record

^{*}For bibliography see references 1 and 2.

FIG. 1. Plan of the array cross section of the detector. Trays containing 24 counters with area: Δ - 330 cm^2 , \circ - 100 cm^2 , and \square - 18 cm^2 each.



pulses over an amplitude range of 10^4 . For work with a small number of chambers, this problem was solved as described in reference 6 by using a linear amplifier and several pulse-height analyzers. In the present array, where the number of recording channels equals 12, non-linear amplifiers are used. In order to widen the range amplitude, the amplification factor for pulses of large amplitude is decreased by means of an additional feedback loop which is connected automatically by the unblocking of a diode, a method used for the first time by Magee, Bell and Jordan.⁷ Recently, this method of widening the dynamic range has become widespread. Three such amplifiers, with an amplification factor of 10 before connecting the additional feedback loop, are used in each of the channels. The amplifiers are designed for amplifying negative pulses and are therefore followed by an inverter with a gain varying from 2 to 4. The pre-amplifier and the pulse-height analyzer are the same as used previously.⁶ The maximum gain of the whole channel is set to be equal to 10^5 for the central region, and to 4×10^5 for the study of the periphery of showers. The accuracy of the output-pulse amplitude measurement depends on the value of the latter. The mean accuracy of the measurement is $\sim 30\%$. The accuracy of measuring small amplitude pulses is limited by the noise which amounts to $\sim \frac{1}{3}$ of the signal produced by the passage of a single relativistic particle through the chamber ($\sim 20 \mu\text{V}$). This makes it possible to measure particle densities in the ionization chambers commencing with $\rho = 0.5 \text{ m}^{-2}$.

The axis location and the number of particles in an individual shower were determined from the values of the charged particle density at various points in the plane of observation. 2000 Geiger-Müller counters with area of 330 cm^2 , 100 cm^2 , and 18 cm^2 were used for measurements of the charged-particle densities. Each counter was connected to a hodoscope cell HK-7. The counters were placed in three enclosures (see Fig. 1). The showers were selected by master systems

placed in each of the enclosures. In the enclosures 1 and 2, the master system gives a signal for each coincidence of signals from six groups of counters with an area of 0.132 cm^2 each. In the enclosure 3, getting an output signal from the master system requires a coincidence of not less than three counters with an area of 100 cm^2 each out of 24 counters placed under 10 cm of lead and of signals from two groups of air counters with an area of 0.26 m^2 (Cocconi core selector). Data on the ionization chambers and hodoscopes is recorded for every signal from the selection systems.

The axes of the showers recorded by the array fell in regions surrounding the selection systems.* In practice, the axes of showers with $N \geq 10^5$ are distributed continuously along the enclosure up to a distance of 60 m from the chambers. Analysis of the hodoscope data is carried out by the usual method,⁹ and makes it possible to determine the total number of particles in the shower N and the distance R from the shower axis to the chamber. For a shower axis falling inside one of the hodoscope points (in an enclosure), the accuracy of determination of N amounts to 20%, and that of R to the order of 1 m.¹⁰ The accuracy becomes worse with increasing distance of shower axis from the line joining the hodoscope points.

RESULTS

All recorded showers were individually analyzed and classified according to the following groups with respect to the number of particles N :

$$N_1 < 1 \cdot 10^4; \quad 1 \cdot 10^4 \leq N_2 < 3 \cdot 10^4; \quad 3 \cdot 10^4 \leq N_3 < 1 \cdot 10^5; \\ 1 \cdot 10^5 \leq N_4 < 3 \cdot 10^5; \quad 3 \cdot 10^5 \leq N_5 < 1 \cdot 10^6 \text{ and } N_6 \geq 10^6.$$

The mean number of particles in each group was determined as follows: $\bar{N}_2 = 2 \times 10^4$; $\bar{N}_3 = 5.6 \times 10^4$; $\bar{N}_4 = 2 \times 10^5$; $\bar{N}_5 = 5.7 \times 10^5$. Showers of each group were then classified with respect

*The size spectrum of showers selected by such systems and their lateral distribution are described in a number of articles (see references 3, 4, and 8).

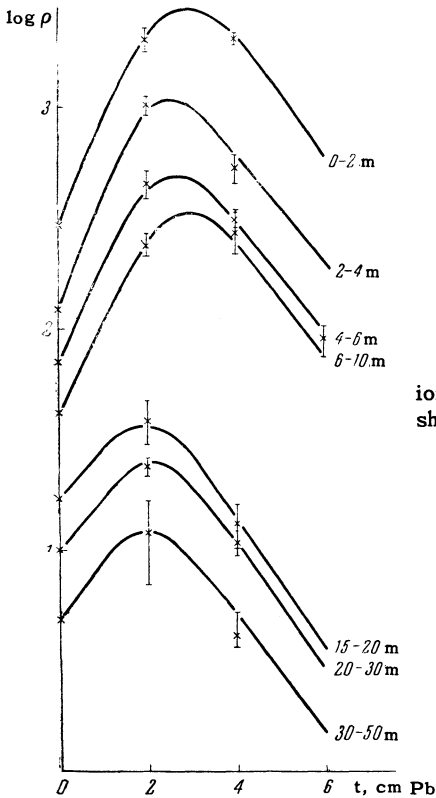


FIG. 2. Transition ionization curves for showers of group N_4 .

to the distance of the axis of each shower from the chamber. A statistical analysis made it possible to find the mean value of the particle density under the lead absorbers of different thickness for each of the distance intervals 0–2; 2–4; 4–6; 6–10; 10–15; 15–20; 20–30; and 30–50 m. Cascade curves for the above distance ranges were then constructed for each \bar{N}_i . At a depth larger than $8t$ (where t is the radiation unit), the curves were constructed using a constant absorption coefficient for photons in lead ($\mu_t = 0.24$). A family of such curves for showers of the group N_4 is shown in Fig. 2. The curves were drawn so that, using a semi-logarithmic scale, they run into straight lines smoothly at $t = 8$.* The energy-flux density ρ_E carried by the electron-photon component was determined from the area under the curves. The integral determining was split into two terms

$$\rho_E = \int_0^{\infty} n(t) \beta dt = \int_0^8 n(t) \beta dt + \int_0^{\infty} \beta n(t=8) \exp(-\mu t) dt.$$

The value of the first term was determined graphically by computing the area under the curves, and the second term from the value of density for $t = 8$.

Data on the energy-flux density of the electron-photon component in showers with different values

*This may, in principle, lead to an underestimate of the energy of the electron-photon component at small distances from the axis (in the range 0–2 m).

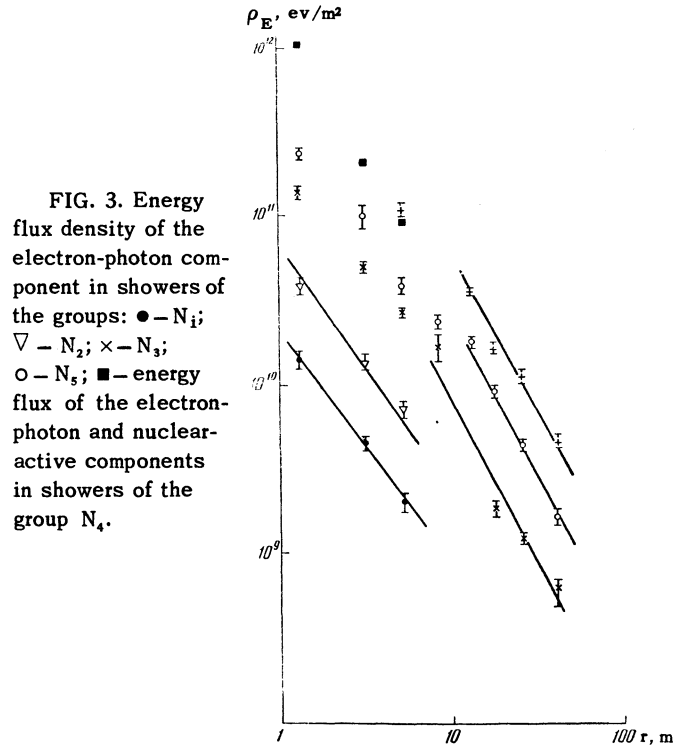


FIG. 3. Energy flux density of the electron-photon component in showers of the groups: \bullet – N_1 ; ∇ – N_2 ; \times – N_3 ; \circ – N_5 ; \blacksquare – energy flux of the electron-photon and nuclear-active components in showers of the group N_4 .

of N as a function of the distance is given in Fig. 3. The role of the nuclear-active component and of μ mesons is discussed below.

The electron lateral-distribution function of a shower is independent of N , and its form has been well studied.¹⁰ Using the data on the energy-flux density and electron density, one can obtain the value of the mean energy carried by one electron in a shower. The values obtained are given in Fig. 4. The values of the mean energy have, within the limits of accuracy, been found to be independent of N , and the data were therefore averaged over all showers.

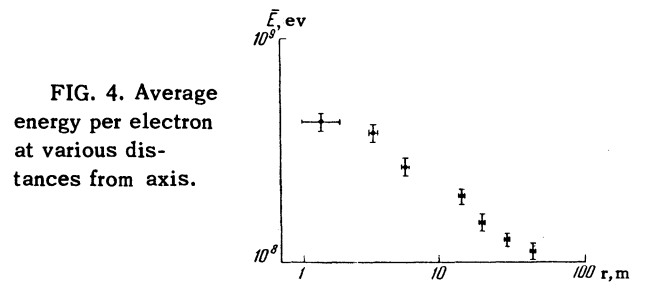


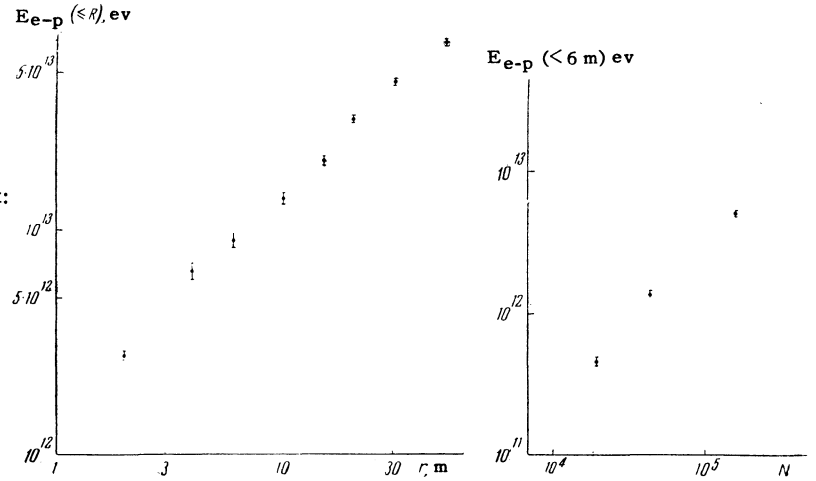
FIG. 4. Average energy per electron at various distances from axis.

If the energy-flux density is known, then it is possible to determine the value of the energy carried by the electron-photon component in a circle of a given radius:

$$E_{e-p}(\leq R, N) = \sum_i \rho_E(r_i, N) \Delta s_i,$$

where the summation is carried over all ranges of the smaller radius. In Fig. 5, the obtained

FIG. 5. Energy of the electron-photon component:
 a — as a function of radius for a shower of the group N_5 ,⁷ b — in a circle with radius $R=6\text{m}$, for different number of particles in the shower.



values of energy in a circle with radius R are given for showers of the group N_5 as a function of the radius. The value of the energy in a circle with radius 6 m for showers with different number of particles is also given in the figure.

In determining the energy of the electron-photon component from ionization under various thicknesses of lead, it is necessary to account for the contribution of the nuclear-active and μ meson components. The energy of the nuclear-active component in the central region of the showers is substantially larger¹⁰ than the energy of the electron-photon component. At distances of the order of 2–4 m from the axis, the energy density of the nuclear-active component is about five times larger than the energy density of the electron-photon component. For larger thicknesses of lead, a large fraction of the energy E_0 of the nuclear-active component is transferred to μ_0 mesons. Using assumptions analogous to those of reference 10, this amounts to $0.03 E_0$ for $t = 4$ cm Pb and to $0.08 E_0$ for $t = 6$ cm Pb. However, the contribution of electrons produced by the π^0 mesons to the total value of ionization is decreased by the fact that the cascades from π^0 mesons have no chance of developing sufficiently in lead since they originate in the depth of the absorber, while the cascades from electrons and photons of the shower start on the boundaries of the absorbers. For the estimate of this factor, the average cascade produced by the first nuclear interaction in lead was calculated. Cascade curves of photons produced by π^0 mesons were approximated, following I. P. Ivanenko,¹¹ by the first three terms of the Laguerre polynomial series. This leads to approximations of the type

$$n(t) = e^{-\gamma t} (at + bt^2 + ct^3).$$

Numerical values of the coefficients were taken from reference 11 for $\epsilon_0 = 118$. It was found that

the number of electrons in such a cascade, for thicknesses of less than 4 cm Pb, decrease by a factor of more than two compared with the number of electrons in the electron-photon cascade of the same energy. Thus, for a lead thickness of 4 cm, only 1 to 1.5% of the energy of the nuclear-active component will, on the average, be added to the electron-photon component determined from the area under the ionization curve up to the depth of 4 cm. With increasing thickness of lead, the contribution of electrons from the nuclear cascade will increase, since the development of the nuclear cascade is much slower than that of the electron-photon cascade.¹² For the estimate of the energy of the electron-photon component, only the data up to 4 cm Pb were used near the shower core. As has been mentioned, beyond 4 cm Pb the curves were drawn with a constant absorption coefficient. It may be seen from the calculation given above that the contribution of the nuclear-active component is then small (less than 10%, even for the central region of showers).

The contribution of the μ mesons component to the energy flux can be estimated in the following way: The total number of μ mesons in the central region of the shower ($R < 6$ m) amounts to 1% of the number of electrons. Hence, the total number of μ mesons in a circle with radius 6 m will be

$$N_\mu = 10^{-2} \int_0^{R=6} \frac{kN}{r} 2\pi r dr = 7.3 \cdot 10^{-4} N,$$

where N is the total number of electrons in the shower, and $k = 2 \times 10^{-3}$. The average contribution of μ mesons to the energy determined from ionization is not larger than the total ionization energy loss of μ mesons, i.e., the loss for the production of δ electrons and for collisions with a small energy loss. For μ mesons of the shower,

$(dE/dx)_{ion} = 2 \times 10^6$ ev/g for lead. Up to the depth of 4 cm, the μ mesons ionization energy loss is therefore given by the formula

$$\Delta E'_\mu = (dE/dx)_{ion} t N_\mu.$$

If one accounts for depths larger than 4 cm Pb, the energy lost by μ mesons increases. For the depths larger than $t = 4$ cm, the curves were continued with a constant slope, and the contribution of μ mesons for such depths is therefore determined from the value of loss for $t = 4$ cm. The total value of the energy due to ionization loss of μ mesons amounts to $E_\mu = 1.1 \times 10^5$ N ev. It may be seen from a comparison with Fig. 5 that

$$\Delta E_\mu (< 6\text{m}) \sim 0.005 E_{e-p} (< 6\text{m}.)$$

At a distance $r \sim 50$ m, the relative number of μ mesons increases by a factor of about two, and the contribution to the ionization produced remains negligible.

DISCUSSION OF RESULTS

The data obtained (see Fig. 3) permits us to state that the form of the lateral distribution function of the electron-photon energy flux is independent of the number of particles in the shower. In the central region of the shower $1 < r < 8$ m, the function may be approximated by a power law with an exponent $n = 1.5 \pm 0.2$, while at distances larger than 10 m, the exponent is $n = -2 \pm 0.3$. Using the log-log scale, the straight lines representing the above relations given in Fig. 3. A comparison of the value obtained for the energy density with the results of the experiments^{3,4} for showers with the same number of particles shows that the data of these experiments are, in this respect, in agreement with our results.

In order to test the agreement of the results with the predictions of the cascade theory, the calculations of the lateral distribution function of the energy flux near the shower axis ($0.5 < r < 6$ m) were carried out by the method given by Guzhavin and Ivanenko.¹³ In reference 13 the integral lateral-distribution functions of electrons of various energies are given for various values of the age parameter s , in addition to the lateral distribution functions of photons of various energies (for $s = 1$); $f_\beta(x, s)$ and $f_\gamma(x, s)$, where $x = Er/E_s$, $E_s = 21.3$ Mev. This made it possible to calculate the mean energy of electrons (and photons) as a function of r , obtaining

$$\begin{aligned} \bar{E}_\beta &= \int_{E_{min}}^{\infty} E \frac{d}{dE} f_\beta(x, s) dE \bigg/ \int_{E_{min}}^{\infty} \frac{d}{dE} f_\beta(x, s) dE \\ &= \frac{E_s}{r} \int_{x_{min}}^{\infty} x f'_\beta(x, s) dx \bigg/ \int_{x_{min}}^{\infty} f'_\beta(x, s) dx. \end{aligned}$$

For an accurate determination of \bar{E} , the lower limit of integration should be made equal to zero. However, the functions f are calculated neglecting ionization loss, and are therefore correct for $E > \beta$. However, a comparison of the electron lateral distribution function with $E \geq 0$ obtained by Nishimura^{1,2} and the curves with the distribution functions of particles with $E \geq E_{min}$ shows that, in the central region of the shower ($r < 6$ m at sea level), the number of particles with $E < E_{min} = 1 \times 10^8$ ev is not larger than 10%. Consequently, the contribution of particles with $E < E_{min}$ to the energy flux carried by the electron photons in that region is smaller than 10%. One can therefore find the mean energy of particles with $E \geq 1 \times 10^8$ ev at various distances and, using the known lateral distribution of electrons and photons with $E \geq 1 \times 10^8$ ev, find the distribution of the energy-flux density with the above accuracy as a function of distance. It should be noted that the values of the mean energy obtained will, in general, be higher. The above mentioned calculations were carried out for three values of s ; $s = 1$, $s = 1.3$, and $s = 1.5$. Since the form of the lateral distribution functions of photons for $s \neq 1$ is not given, we assume then, for $s = 1.3$ and 1.5 , that the ratio of the mean energies of electrons and photons for different values of s is the same as $s = 1$.

It was found that, at distances $0.5 \leq r < 6$ m in a shower characterized by the value $s = 1$, this function can be approximated by a power function with the exponent $n = -1.73$. For $s = 1.3$, the exponent is $n = -1.6$; while, for $s = 1.5$, it is $n = -1.45$. One can therefore maintain that the data on the lateral distribution of the energy flux of the electron-photon component do not contradict the value of the parameter $s = 1.2$ obtained for the average shower from the form of the lateral distribution function. A comparison of the obtained data with the results of investigations^{8,10} shows directly that the energy-flux distribution of the nuclear-active component is much narrower than the energy flux of the electron-photon component.

The value of the average energy given in Fig. 4 was also compared with the results of our calcu-

lations (see above). It was found that, for $s = 1.3$, the average energy per electron as a function of distance in the same region of the shower can be described by a power law with an exponent $n = -0.65$. It was found experimentally that the average energy changes at a slower rate, $n \approx -0.5$, and that, the value of the average energy is markedly less than that calculated for $r = 3$ m (by a factor of 2.5). However, as has been stated above, the average energy near the shower axis may be slightly underestimated, and the calculated value overestimated.

To compare our results with those of Matano et al.,⁵ Fig. 3 includes points (squares) corresponding to the total energy flux of the two components (nuclear-active and electron-photon) near the axis of a shower with $\bar{N} = 2 \times 10^5$. Data on the energy flux of the nuclear-active component are taken from reference 10. The decrease of the total energy flux near the shower axis can be described by a power function with $n = -2.0$. The value of the energy obtained by us for $r = 5$ m agrees closely with the data of reference 5, but the increase of the energy density near the axis given there is steeper. However, Matano et al. did not carry out an analysis of individual showers. Instead, the axis location of showers was estimated from the value of the mean energy observed in each case. If a spread of energy values at a given distance existed in the real shower, then such a method would lead to steeper increase of energy near the shower axis. In our experiment, we determined the place of incidence of the shower independently, and therefore, in principle, obtained the average value of the energy at a given distance from the axis.

The values of the electron-photon component in a circle with radius $R = 6$ m given in Fig. 5 show that the energy flux is proportional to the total number of particles in the shower N . Data on the energy of electron-photon component in a circle with a radius of 50 m are also given in Fig. 5. However, only a little over half of the shower particles is contained in such a circle. It follows from Fig. 4 that the average energy per electron at distances larger than 50 m is smaller than 10^8 ev. Assuming that for large distances $\bar{E} = \beta$, we find that 70–80% of the total energy of the electron-photon component is contained in a circle with $R = 50$ m. If we represent the energy carried by the electron-photon component by the expression $E_{e-p} = aN$, then $a \approx 1.7 \times 10^8$ ev $\approx 2.5 \beta$.

CONCLUSIONS

1. The form of the lateral distribution function of the energy flux of the electron-photon component of EAS has been obtained. The function is a power law with the following exponents:

$$n = -1.5 \pm 0.2 \text{ for } 1 \text{ m} < r < 8 \text{ m,}$$

$$n = -2.0 \pm 0.3 \text{ for } 10 \text{ m} < r < 50 \text{ m.}$$

2. It was found that the lateral distribution function of the energy of the electron photon component in showers with total number of particles $N = 10^4 - 10^6$ is independent of the shower size.

3. The lateral distribution of the energy flux of the electron-photon component is not in disagreement with the theoretical distribution obtained from the cascade theory for $s = 1.2$.

4. About 75% of the total energy of the electron-photon of EAS is contained in a circle with 50 m radius.

The authors would like to thank S. N. Vernov and G. T. Zatsepin for their great help, and I. P. Ivanenko for discussion of the results obtained. They would also like to thank V. I. Artemkin, L. A. Dikarev, V. N. Sokolov, K. I. Solov'ev, and D. S. Stel'makh, who took part in the measurements and in the analysis of the data.

¹K. Greisen, Progress in Cosmic Ray Physics **3**, Amsterdam, 1956.

²G. Cocconi, Handbuch der Physik **45**, 1958.

³Ivanovskaya, Kulikov, Rakobol'skaya, and Sarycheva, J. Exptl. Theoret. Phys. (U.S.S.R.) **33**, 358 (1958), Soviet Phys. JETP **6**, 276 (1958).

⁴Danilova, Dovzhenko, Nikol'skiĭ, and Rakobol'skaya, J. Exptl. Theoret. Phys. (U.S.S.R.) **34**, 541 (1958), Soviet Phys. JETP **7**, 374 (1958).

⁵Matano, Miura, Oda, Suga, Tanahashi, and Tanaka, Nuovo cimento **8**, Suppl. 2, 668 (1958).

⁶Bekkerman, Dmitriev, Molchanov, Khristiansen, and Yarigin, Приборы и техника эксперимента (Instruments and Meas. Engg.), No. 4 (1958).

⁷Magee, Bell, and Jordan, Rev. Scient. Instr. **23**, 30 (1952).

⁸Dmitriev, Kulikov, and Khristiansen, Nuovo cimento **8**, Suppl. 2, 587 (1958).

⁹Abrosimov, Goryunov, Dmitriev, Solov'eva, Khrenov, and Khristiansen, J. Exptl. Theoret. Phys. (U.S.S.R.) **34**, 1077 (1958), Soviet Phys. **7**, 746 (1958).

¹⁰Abrosimov, Dmitriev, Kulikov, Massal'skiĭ, Solov'ev, and Khristiansen, J. Exptl. Theoret.

Phys. (U.S.S.R.) **36**, 751 (1958), Soviet Phys. JETP **9**, 528 (1959).

¹¹ I. P. Ivanenko, Dokl. Akad. Nauk SSSR **107**, 819 (1956), Soviet Phys. "Doklady" **1**, 231 (1956).

¹² Zatsepin, Krugovykh, Nikol'skiĭ, and Murzina, J. Exptl. Theoret. Phys. (U.S.S.R.) **34**, 298 (1958), Soviet Phys. JETP **7**, 207 (1958).

¹³ V. V. Guzhavin and I. P. Ivanenko, Dokl. Akad. Nauk SSSR **113**, 533 (1957); **115**, 1089 (1957), Soviet Phys. "Doklady" **2**, 131 (1957); **2**, 407 (1957).

Translated by H. Kasha
197